Available online at www.sciencedirect.com
SCIENCE DIRECT
Journal of Organometallic Chemistry 691 (2006) 193–201
Journal of Organometallic Chemistry
www.elsevier.com/locate/jorganchem

Stereospecific polymerization of propylene with group 4 *ansa*-fluorenylamidodimethyl complexes

Kei Nishii [a], Hideaki Hagihara [b], Tomiki Ikeda [a], Munetaka Akita [a], Takeshi Shiono [c,*]

[a] *Chemical Resources Laboratory, Tokyo Institute of Technology, Nagatsuta-cho 4259, Midori-ku, Yokohama 226-8503, Japan*
[b] *Macromolecular Technology Research Center, National Institute of Advanced Industrial Science and Technology, Central 5, 1-1-1 Higashi, Tsukuba, 305-8565 Japan*
[c] *Department of Applied Chemistry, Graduate School of Engineering, Hiroshima University, Kagamiyama 1-4-1, Higashi-Hiroshima 739-8527, Japan*

Received 18 April 2005; received in revised form 2 August 2005; accepted 9 August 2005
Available online 27 September 2005

Abstract

Group 4 [η^1:η^3-*tert*-butyl(dimethylfluorenylsilyl)amido]dimethyl complexes [*t*-BuNSiMe$_2$Flu]MMe$_2$ (M = Ti, **1**; Zr, **2**; Hf, **3**) were synthesized in a one-pot synthesis starting from the ligand, MeLi and MCl$_4$ (M = Ti, Zr, Hf), respectively. The structures of these complexes were determined by X-ray crystallography and the results obtained revealed that the fluorenyl ligand coordinates to center metal in a η^3-manner irrespective of center metal employed. Propylene polymerization was conducted at 0 or 20 °C in toluene by **1**–**3** combined with dried methylaluminoxane (MAO), which was prepared from the toluene solutions of MAO by removing free trialkylaluminiums, and HNMe$_2$PhB(C$_6$F$_5$)$_4$ in the presence of triisobutylaluminium. The **1**–dried MAO system gave the polymer with syndiotactic triad (rr) of 63% at 0 °C, whereas **2** and **3** did not give any polymer in the same conditions. The **2**–dried MAO system gave the polymer with the highest syndiotacticity (rr = 97%) at 20 °C, although the activity was low. The **3**–dried MAO system did not give any polymer even at 20 °C. When HNMe$_2$PhB(C$_6$F$_5$)$_4$ was used in place of dried MAO at 20 °C, **1** gave almost atactic polymer, while **2** and **3** gave highly syndiotactic one (rr > 90%). These results indicate that the catalytic performance strongly depended on the center metal of the *ansa*-fluorenylamidodimethyl complexes as well as cocatalysts employed.

Keywords: Syndiotactic; Atactic; Metallocene catalysts; Polypropylene

1. Introduction

Since the discovery of metallocene catalysts, a great number of organometallic compounds have been applied for olefin polymerization as so-called single-site catalysts from both the academic and the industrial points of view [1]. During the first half of the 1990's, Bercaw [2], Okuda [3], the researchers of Dow [4] and Exxon [5] reported a new type of half metallocene complexes which contain the N-based ligand attached to the cyclopentadiene derivatives, named *ansa*-monocyclopentadienylamido (CpA) complex [1c,6]. The CpA complexes have been found to be highly efficient catalysts for synthesis of linear low-density polyethylene and copolymerization of ethylene and styrene [4,5,7]. Several researchers reported the synthesis of a series of group 4 CpA complexes and the influence of the ligand in CpA complexes on the stereospecificity and the regiospecificity of propylene polymerization [8]. Okuda et al. [9] prepared *tert*-butylamidofluorenylzirconium complexes for potentially syndiospecific catalyst. We have found that [*t*-BuNSiMe$_2$Flu]TiMe$_2$ (**1**) activated with methylaluminoaxane (MAO), B(C$_6$F$_5$)$_3$ or Ph$_3$CB(C$_6$F$_5$)$_4$ promoted the polymerization of propylene at 40 °C in syndiospecific and highly regiospecific manner [10]. Razavi et al. and Busico et al. reported the introduction of *tert*-butyl group on the fluorenyl ligand ([*t*-BuNSiMe$_2$(2,7-di-*t*-Bu-Flu)]TiCl$_2$, [*t*-BuNSiMe$_2$(3,6-di-*t*-Bu-Flu)]TiCl$_2$) increased the syndiospecificity and activity [11].

* Corresponding author. Tel.: +81 82 424 7730; fax: +81 82 424 5494.
E-mail address: tshiono@hiroshima-u.ac.jp (T. Shiono).

0022-328X/$ - see front matter © 2005 Elsevier B.V. All rights reserved.
doi:10.1016/j.jorganchem.2005.08.027

Shiomura et al. [12] reported that the activation of [*t*-BuNSiMe$_2$Flu]ZrCl$_2$ with MAO-^{i}Bu$_3$Al gave syndiotactic polypropylene (PP) ([rrrr] = 77%), whereas the activation with Ph$_3$CB(C$_6$F$_5$)$_4$-^{i}Bu$_3$Al gave isotactic PP ([mmmm] = 95%). Recently, Fujita et al. [13] reported that the nature of the center metal had a significant effect on catalytic performance and the microstructures of produced PPs using group 4 bis(phenoxy-imine) complex-based catalysts. These results indicate that stereoregularity of PPs obtained should be controlled by the kinds of counter anion and the kinds of center meal.

We have previously reported that **1** activated with B(C$_6$F$_5$)$_3$ produced syndiotactic-enriched PP at −50 °C in a living manner [14a] and the replacement of B(C$_6$F$_5$)$_3$ with trialkylaluminium(Me$_3$Al, ^{i}Bu$_3$Al)–free MAO, named dried MAO and dried modified MAO (MMAO), raised the living polymerization temperature up to 0 °C accompanied by the improvement of syndiospecificity [14b,14c]. These results suggest that stereospecificity and propylene polymerization behavior in the complex **1**-based catalysts strongly depend on the cocatalyst and polymerization conditions employed.

In this paper, we synthesized a series of group 4 *ansa*-fluorenylamidodimethyl complexes by applying the synthetic method reported by Resconi et al. [15] and investigated the effects of center metal and cocatalyst on the catalytic performance of propylene polymerization.

2. Experimental part

2.1. Materials

Dimethylaniliniumtetrakis(pentafluorophenyl)borate (HNMe$_2$PhB(C$_6$F$_5$)$_4$) and toluene solution of MAO were donated from Tosoh-Finechem Co. Ltd. Dried MAO was prepared from the toluene solution of MAO by vacuum drying followed by washing with hexane as reported previously [14b]. Research grade propylene (Takachiho Chemicals Co.) was purified by passing it through columns of NaOH, P$_2$O$_5$, and molecular sieves 3A, followed by bubbling it through a NaAlH$_2$Et$_2$/1,2,3,4-tetrahydronaphthalene solution. All solvents were commercially obtained and dried with standard methods.

2.2. Synthesis of t-BuNHSiMe$_2$Flu (Flu = C$_{13}$H$_9$) ligand

All the syntheses were carried out under N$_2$ by standard Schlenk techniques. The *t*-BuNHSiMe$_2$Flu ligand was prepared according to the literature (Scheme 1) [9,16]. To a solution of fluorene (24 g, 144 mmol) in Et$_2$O (300 mL) was added *n*-butyl lithium (96 mL, 1.50 M solution in hexane, 144 mmol) at 0 °C within 1 h. After stirring for 3 h at room temperature, the solvent was removed in vacuo to give Li[Flu]. To a solution of excess dichlorodimethylsilane (40 mL) was added the suspension of Li[Flu] in hexane (250 mL) at −78 °C. The resultant suspension was stirred for 8 h at room temperature, and the solvent and the remained dichlorodimethylsilane were removed in vacuo. After the addition of hexane (150 mL), lithium chloride was precipitated and the solution was decanted, followed by removal of the solvent, 34.2 g (132 mmol) of 9-(chlorodimethylsilyl)fluorene was obtained as off-white solid.

To a solution of 9-(chlorodimethylsilyl)fluorene 34.2 g (132 mmol) in THF (200 mL) was added *t*-butylamine (20 mL, 264 mmol) at 0 °C. Stirring overnight at room temperature gave a yellow-orange suspension. Lithium chloride was precipitated and the solution was decanted. Removal of the solvent gave *t*-BuNHSiMe$_2$Flu as yellow oil (28.5 g, 96.5 mmol, 67% yield). ^{1}H NMR (C$_6$D$_6$, ref. C$_6$H$_6$: 7.15 ppm): δ = 7.79 (d, 2H, C$_{13}H_9$), 7.61 (d, 2H, C$_{13}H_9$), 7.29 (dd, 4H, C$_{13}H_9$), 3.76 (s, 1H, C$_{13}H_9$), 1.02 (s, 9H, C(CH_3)$_3$), 0.42 (s, 1H, N*H*), −0.09 (s, 6H, Si(CH_3)$_2$).

2.3. Synthesis of [t-BuNSiMe$_2$Flu]TiMe$_2$ (**1**)

To a solution of *t*-BuNHSiMe$_2$Flu (1.56 g, 5.28 mmol) in Et$_2$O (50 mL) was slowly added excess MeLi (24.0 mL of a 1.20 M solution in Et$_2$O, 28.2 mmol) at room temperature and the mixture was stirred for 5 h. To TiCl$_4$ (0.58 mL, 5.29 mmol) diluted with 50 mL of pentane was added a solution of the dilithium salt in Et$_2$O at room temperature. The resulting dark brown suspension was stirred overnight at room temperature. After the solvent was removed, the residue was extracted with hexane (120 mL) and the hexane solution was decanted. To the hexane solution was added MeMgBr (3.0 mL of a 3.0 M solution in Et$_2$O), and the resulting mixture was stirred for 5 h at room temperature. After the solvent was removed, the residue was extracted with hexane (80 mL). The hexane solution was concentrated and cooled overnight at −30 °C to give **1** (route I in Scheme 1) as yellow-orange microcrystals (0.840 g, 2.26 mmol, 42.8%). ^{1}H NMR (C$_6$D$_6$): δ = 7.82 (dd, 2H, C$_{13}H_8$), 7.67 (dd, 2H, C$_{13}H_8$), 7.22 (ddd, 2H, C$_{13}H_8$), 7.09 (ddd, 2H, C$_{13}H_8$), 1.37 (s, 9H, C(CH_3)$_3$), 0.67 (s, 6H, SiCH_3), −0.02 (s, 6H, TiCH_3). ^{13}C NMR (C$_6$D$_6$): δ = 135.0, 129.2, 127.8, 127.7, 124.8, 123.7 (*C*$_{13}$H$_8$), 58.6 (*C*(CH$_3$)$_3$), 56.7 (Ti(*C*H$_3$)$_2$), 34.3 (C(*C*H$_3$)$_3$), 5.7 (Si(*C*H$_3$)$_2$). Anal. Calc. for C$_{21}$H$_{29}$NSiTi: C, 67.91; H, 7.87; N, 3.77. Found: C, 68.03; H, 7.87; N, 3.89.

2.4. Synthesis of [t-BuNSiMe$_2$Flu]ZrMe$_2$ (**2**)

The same procedure for the preparation of **1** was applied except ZrCl$_4$ was used in the final step. The hexane solution was concentrated and cooled overnight at −30 °C to give **2** as yellow microcrystals (yield, 42.4%). ^{1}H NMR (C$_6$D$_6$): δ = 7.77–7.80 (m, 4H, C$_{13}H_8$), 7.13–7.16 (m, 4H, C$_{13}H_8$), 1.29 (s, 9H, C(CH_3)$_3$), 0.74 (s, 6H, SiCH_3), −0.58 (s, 6H, ZrCH_3). ^{13}C NMR (C$_6$D$_6$): δ = 136.2, 128.7, 125.7, 124.2, 123.8 (*C*$_{13}$H$_8$), 55.6 (*C*(CH$_3$)$_3$), 41.4 (Zr(*C*H$_3$)$_2$), 34.9 (C(*C*H$_3$)$_3$), 7.0 (Si(*C*H$_3$)$_2$). EI-MS: m/z = 413 (M$^+$).

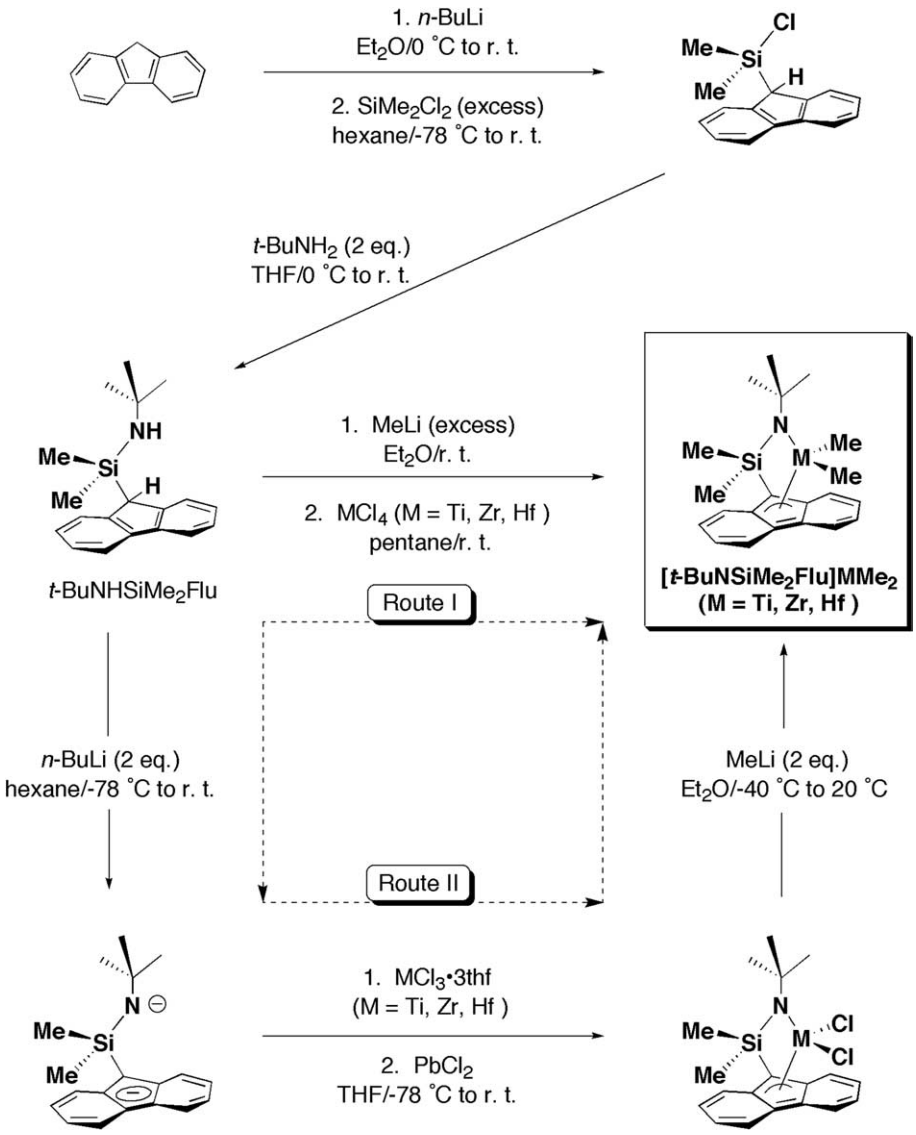

Scheme 1. Synthetic procedure for group 4 *ansa*-fluorenylamidodimethyl complexes.

2.5. Synthesis of [t-BuNSiMe$_2$Flu]HfMe$_2$ (3)

The same procedure for the preparation of **1** was applied except $HfCl_4$ was used in the final step. The hexane solution was concentrated and cooled overnight at −30 °C to give **3** as light-yellow needle crystals (yield, 42.2%). ^{1}H NMR (C_6D_6): $\delta = 7.78$–7.80 (m, 4H, $C_{13}H_8$), 7.14–7.16 (m, 4H, $C_{13}H_8$), 1.26 (s, 9H, $C(CH_3)_3$), 0.77 (s, 6H, $SiCH_3$), −0.80 (s, 6H, $HfCH_3$). ^{13}C NMR (C_6D_6): $\delta = 136.6$, 128.9, 125.5, 124.1, 123.8 ($C_{13}H_8$), 72.8 (C9 of $C_{13}H_8$), 54.8 ($C(CH_3)_3$), 51.4 ($Hf(CH_3)_2$), 35.3 ($C(CH_3)_3$), 7.0 ($Si(CH_3)_2$). EI-MS: $m/z = 502$ (M^+).

2.6. Polymerization procedure

Polymerization was performed in a 100-mL glass reactor equipped with a magnetic stirrer as follows. Toluene as solvent was placed in the reactor. After the solvent was saturated with gaseous propylene under atmospheric pressure, polymerization was started by successive addition of prescribed amounts of cocatalyst and catalyst. The propylene pressure and temperature were kept constant during the polymerization. Polymerization was conducted for a prescribed time, and quenched by addition of HCl/methanol solution. The polymers obtained were adequately washed with methanol and dried under vacuum at 60 °C for 6 h.

2.7. Analytical procedures

Molecular weight and molecular weight distribution of PPs obtained were determined by gel permeation chromatography (GPC) with a Waters 150 CV at 140 °C using *o*-dichlorobenzene as a solvent. The parameters for universal calibration were $K = 7.36 \times 10^{-5}$, $\alpha = 0.75$ for polystyrene standard and $K = 1.03 \times 10^{-4}$, $\alpha = 0.78$ for PP sample.

The ^{1}H NMR spectra of complexes were measured at room temperature on a JEOL GX500 spectrometer operated at 500.00 MHz in pulse Fourier-transform mode.

The pulse angle was 45° and 64 scans were accumulated in pulse repetition of 7.0 s. The ^{13}C NMR spectra of PPs were measured at 120 °C on a JEOL GX 500 spectrometer operated at 125.65 MHz in the pulse Fourier-transform mode. The pulse angle was 45° and about 5000 scans were accumulated in pulse repetition of 5.0 s. Sample solutions were prepared in 1,1,2,2-tetrachloroethane-d_2 up to 10 wt%. The central peak of 1,1,2,2-tetrachloroethane (74.47 ppm) was used as an internal reference.

EI-MS (electron impact mass spectrum) was recorded on a JEOL JMS-SX 102A mass spectrometer at 30 eV.

Differential scanning calorimetry (DSC) analysis was performed on a Seiko DSC-220. The samples were encapsulated in aluminum pans and annealed at 80 °C for 4 h to ensure sufficient time for crystallization. After annealing, the DSC curves of the samples were recorded under a nitrogen atmosphere with a heating rate of 10 °C/min from 20 to 200 °C.

2.8. X-ray structure determination

Single crystals were mounted on glass fibers. Diffraction measurements were made on a Rigaku RAXIS IV imaging plate area detector with Mo Kα radiation ($\lambda = 0.71069$ Å). Indexing was performed from 2 oscillation images, which were exposed for 5 min. The crystal-to-detector distance was 110 mm. Readout was performed with the pixel size of 100 μm × 100 μm. Neutral scattering factors were obtained from the standard source [17]. In the reduction of data, Lorentz and polarization corrections and empirical absorption corrections were made [18].

The structural analysis was performed on an IRIS O2 computer using TEXSAN structure solving program system obtained from the Rigaku Corp., Tokyo, Japan [19]. The structures were solved by a combination of the direct methods (SHELXS-86) [20] and Fourier synthesis (DIRDIF-94) [21]. Least-squares refinements were carried out using SHELXL-97 [20] (refined on F^2) linked to TEXSAN. All the non-hydrogen atoms were refined anisotropically. The methyl hydrogen atoms except the hydrogen atoms attached to the carbon atoms sitting on a crystallographic mirror plane, were refined using riding models, and the other hydrogen atoms were fixed at the calculated positions.

3. Results and discussion

3.1. Synthesis and crystal structures of complexes

The synthetic routes of dimethylfluorenylsilylamine ligand and its complexation with group 4 metal are summarized in Scheme 1.

The reaction of $Me_2Si(FluH)Cl$ ($Flu = C_{13}H_8$) with excess *tert*-$BuNH_2$ [6,16] in THF at room temperature afforded the ligand, *t*-$BuNHSiMe_2FluH$ [9], in a high yield, as described in the experimental section.

The route II in Scheme 1 is the conventional three-step synthetic procedure for the syntheses of group 4 *ansa*-fluorenylamidodimethyl complexes [5c,10,22].

Resconi et al. have recently reported the synthesis of group 4 metallocene dimethyl complexes [15b] and CpA dimethyl complexes [15a] from the ligand, a 2-fold excess of MeLi and MCl_4 (M = Ti, Zr, Hf), in a one-pot synthesis as shown by route I in Scheme 1.

We applied this method for the synthesis of group 4 *ansa*-fluorenylamidodimethyl complexes and could isolate [*tert*-butyl(dimethylfluorenylsilyl)amido]dimethyl complexes [*t*-$BuNSiMe_2Flu]MMe_2$ (M = Ti (**1**), Zr (**2**), Hf (**3**)) as yellow-orange microcrystals of **1**, yellow microcrystals of **2** and light-yellow needle crystals of **3**, respectively.

^1H NMR spectra of **1**, **2** and **3** show that the methyl groups bonded to Si and transition metal atoms are equivalent, respectively. The result suggests that N atom is trigonal planar and all complexes are C_s-symmetric in C_6D_6 solution. The single-crystal X-ray diffraction analysis of **1**, **2**, and **3** were performed, and the structures obtained are displayed in Figs. 1–3, respectively. Crystallographic data and parameters are listed in Table 1. Selected bond lengths and angles are given in Table 2.

The bond lengths: Ti(1)–C(3), Ti(1)–C(4), Ti(1)–C(5), Ti(1)–C(6) and Ti(1)–C(7) of tetramethylcyclopentadienylamidodimethyltitanium complex ([*t*-$BuNSiMe_2Cp^*]TiMe_2$) [23] and heterocycle-fused-indenylsilylamidodimethyltitanium complex ([*t*-$BuNSiMe_2$(*N*-Et-5,6-dihydroindeno[2,1-*b*]indol-6-yl)]$TiMe_2$) [15c], in which the Cp* and indenyl group coordinate to the Ti atom with a η^5-manner, are ranging from 2.283 to 2.463 Å and from 2.271 to 2.557 Å, respectively. The Ti(1)–C(6) and Ti(1)–C(7) lengths of **1** are about 0.110 Å longer than those of the Cp* complex, and 0.015–0.032 Å longer than those of the heterocycle-fused indenyl complex. The results suggest that the Flu ligand in **1** should coordinate to the Ti atom in a η^3-manner rather than in a η^5-manner. Chart 1 shows various bonding modes of Flu ligands found in ansa and simple metallocenes by X-ray diffraction studies [24], which are the mode η^5 bonded to the five-membered ring of the Flu

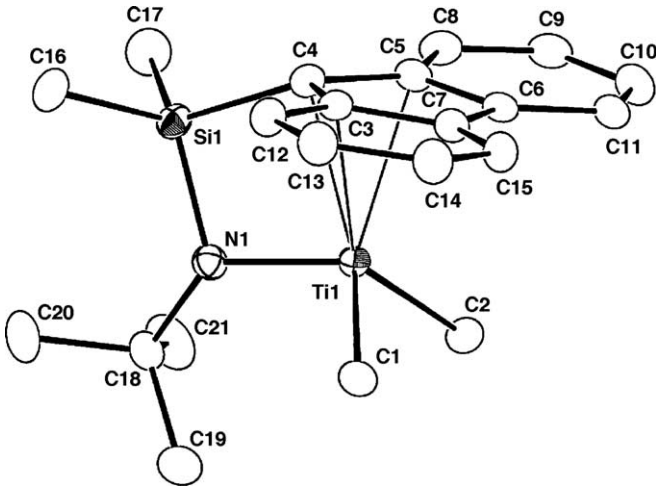

Fig. 1. ORTEP drawing of **1**. Hydrogen atoms are omitted for clarity. The thermal ellipsoids are drawn at the 30% probability level.

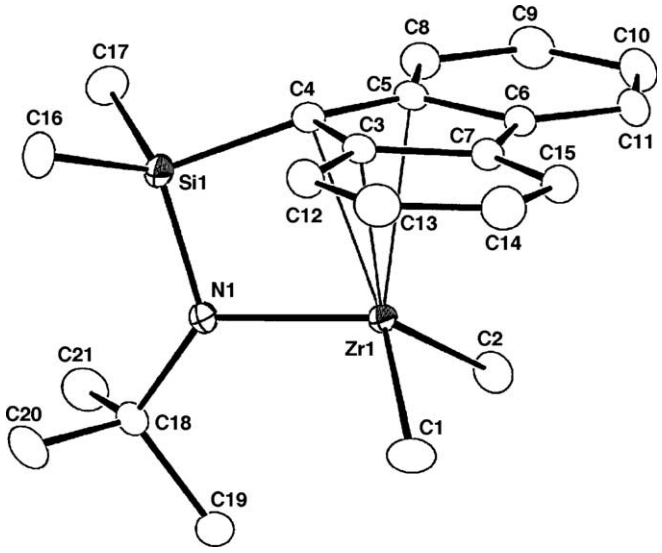

Fig. 2. ORTEP drawing of **2**. Hydrogen atoms are omitted for clarity. The thermal ellipsoids are drawn at the 30% probability level.

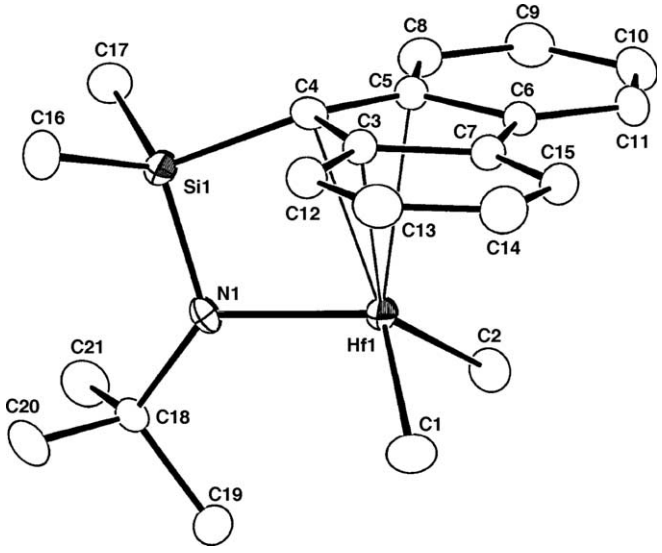

Fig. 3. ORTEP drawing of **3**. Hydrogen atoms are omitted for clarity. The thermal ellipsoids are drawn at the 30% probability level.

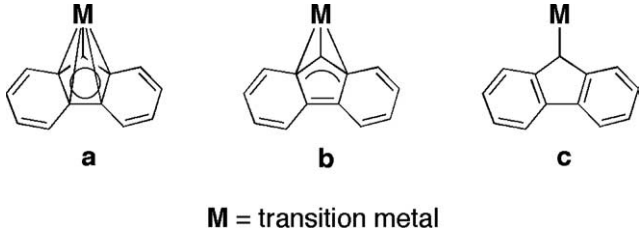

Chart 1. Bonding modes of complexes that contains the fluorenyl ligand.

ligand (**a**), η^3 bonded (**b**), e.g., in (η^5:η^3-CpSiMe$_2$Flu)-YCl$_2$Li(OEt$_2$)$_2$ [25] and (η^5:η^3-Flu)$_2$Sm(THF)$_2$ [26], and symmetrically η^1 bonded (**c**) as in Me$_2$Si(η^1-Flu′)(η^1-*N*-*t*-Bu)ZrCl$_2$OEt$_2$ (Flu′ = C$_{29}$H$_{36}$) [27].

The molecular structure of **2** was similar to that of [*t*-BuNSiMe$_2$Flu]Zr(SiMe$_3$)$_2$ [9], [*t*-BuNSiMe$_2$Flu]ZrCl$_2$ [28] and [*t*-BuNSiMe$_2$(3,6-di-*t*-Bu-Flu)]ZrCl$_2$ [11b], in which the Flu group coordinate to the zirconium atom with a η^5-manner. Okuda et al. suggested that the Flu ligand was bonded in a fashion between η^5 and η^3, as judged by Zr ring-carbon distances ranging from 2.400 to 2.708 Å in [*t*-BuNSiMe$_2$Flu]Zr(SiMe$_3$)$_2$. The bond lengths of Zr(1)–C(6) and Zr(1)–C(7) in **2** are about 0.058 or 0.035 Å longer than those of [*t*-BuNSiMe$_2$Flu]ZrCl$_2$ and [*t*-BuNSiMe$_2$(3,6-*t*-Bu$_2$-Flu)]ZrCl$_2$. Meunier et al. and Rieger et al. have recently reported that the Flu group coordinates to the Zr atom with a η^3-manner in [Me$_2$Si(isodicyclopentadienyl)(Flu)]ZrCl$_2$ [29a] or *rac*-[Et-(Flu)(2-MeBenz[*b*]indeno[4,5-*d*]thiophen-1-yl)]ZrCl$_2$ [29b], in which the Zr–C lengths are ranging from 2.408 to 2.763 Å or from 2.404 to 2.696 Å. Considering the complexes described above, the coordination mode of **2** could be also a η^3-manner.

As compared **2** with **3**, the Zr(1)–C(1,2) lengths are ca. 0.021 Å longer than the Hf(1)–C(1,2) lengths. Other differences can probably be neglected. The results described above suggested that reduced hapticity (η^3) of the Flu ligand in **1**–**3** are retained in the single-crystal state.

The bond angles of N(1)–M(1)–C(4) in **1** is larger than those of **2** and **3**. The result suggests that **1** should present the most open space for the catalytic active site among the three complexes.

3.2. Polymerization of propylene activated with dried MAO

Propylene polymerization was conducted at 0 and 20 °C in toluene by **1**–**3** combined with dried MAO. The results are summarized in Table 3.

The complex **1** combined with dried MAO gave PP with the highest activity at 0 °C. We have previously reported that the system conducted syndiospecific polymerization in a living manner [14b]. On the other hand, **2** and **3** did not give any polymer in the same conditions. The ^{13}C NMR spectrum of the methyl region of PP obtained is shown in Fig. 4(a).

The triad analysis showed that the produced polymer with **1** was syndiotactic-enriched (rr = 63%) as reported previously [14b].

The polymerization with **2** was, therefore, conducted at 20 °C. Although the activity was low, the produced PP was highly syndiotactic (rr = 97% in Fig. 4(b)) with the melting temperature of 124 °C. In addition, the signals arising from regioerror units were not observed in the NMR spectrum of **2** similarly to that of **1**. Although the complex **2** that possesses the non-substituted Flu ligand activated with dried MAO system showed the low polymerization activity, Miller et al. recently reported that the steric expanded zirconium Flu-amido complex (Me$_2$Si(η^1-Flu′)(η^1-*N*-*t*-Bu)ZrCl$_2$ · OEt$_2$, Flu′ = C$_{29}$H$_{36}$)–MAO system showed high activity for propylene polymerization and gave the highly syndiotactic polymer with the highest melting point reported so far [27].

Table 1
Crystallographic data and parameters for **1**, **2** and **3**

	1 (Ti)	**2** (Zr)	**3** (Hf)
Formula	$C_{21}H_{29}NSiTi$	$C_{21}H_{29}NSiZr$	$C_{21}H_{29}NSiHf$
Formula weight	371.45	414.77	502.04
Crystal system	Monoclinic	Orthorhombic	Orthorhombic
Space group	*C*2/*c*	*Pnma*	*Pnma*
a (Å)	24.707(4)	8.3517(3)	8.3597(3)
b (Å)	12.215(2)	14.4219(5)	14.436(1)
c (Å)	14.293(7)	16.8132(6)	16.869(1)
β (°)	113.176(4)		
V (Å^3)	3965(1)	2025(1)	2035(1)
Z	8	4	4
F(000)	1584	864	992
D_{calc} (g · cm^{-3})	1.244	1.360	1.638
μ (mm^{-1})	0.494	0.604	5.176
Max. 2*θ* (°)	55	55	55
No. of reflections observed	4280	15808	15843
No. of parameters refined	333	177	121
R_1[a]	0.0563	0.0361	0.0430
wR_2[b]	0.1595	0.1010	0.1249
No. of obsd. reflns. ($I > 2\sigma(I)$)	3860	2096	2222

[a] $R_1 = [\sum||F_o| - |F_c||]/\sum|F_o|$.
[b] $wR_2 = [\sum[w(F_o^2 - F_c^2)^2]/\sum[w(F_o^2)_2]]^{1/2}$.

Table 2
Selected bond lengths (Å) and angles (°) for **1**, **2** and **3**

	1 (Ti)	**2** (Zr)	**3** (Hf)
Lengths			
M(1)–C(1)	2.105(3)	2.244(3)	2.223(6)
M(1)–C(2)	2.106(3)	2.244(3)	2.223(6)
M(1)–C(3)	2.415(3)	2.529(2)	2.515(3)
M(1)–C(4)	2.253(3)	2.404(3)	2.401(5)
M(1)–C(5)	2.418(3)	2.529(2)	2.515(3)
M(1)–C(6)	2.572(3)	2.672(2)	2.664(3)
M(1)–C(7)	2.573(3)	2.672(2)	2.664(3)
M(1)–N(1)	1.923(3)	2.063(2)	2.046(4)
M(1)–Si(1)	2.836(1)	2.989(7)	2.967(1)
Angles			
N(1)–M(1)–C(4)	78.3(10)	72.9(9)	73.9(2)
M(1)–N(1)–Si(1)	101.0(1)	103.6(1)	103.0(2)
N(1)–Si(1)–C(4)	94.2(1)	95.7(1)	96.1(2)

The *N* value in entry 3 was 3.6 times higher than the number of the Zr complex employed. Since the signals arising from vinylidene and *n*-propyl chain end groups (Fig. 4(b)) were observed in the polymer obtained by the **2** system, we can conclude β-H elimination from the propagating chain to the Zr species or propylene monomer occurred. The complex **3** activated with dried MAO did not give any polymer, even when polymerization was conducted at 20 °C.

3.3. Polymerization of propylene activated with $HNMe_2PhB(C_6F_5)_4$

Propylene polymerization with **1**–**3** was investigated using $HNMe_2PhB(C_6F_5)_4$ as a cocatalyst in the presence of $^iBu_3Al$ at 20 °C in toluene under atmospheric pressure. The polymerization results are summarized in Table 4.

Table 3
Results of propylene polymerization with [*t*-BuNSiMe$_2$Flu]MMe$_2$–dried MAO catalysts[a]

Entry	Catalyst	Temperature (°C)	*A*[b]	M_n[c] (×10^3)	M_w/M_n[c]	*N*[d] (μmol)	rr[e] (%)	T_m[f] (°C)
1	**1** (Ti)[g]	0	257	157	1.22	16	63	–[h]
2	**2** (Zr)	0	–[i]	–	–	–	–	–
3	**2** (Zr)	20	11	1.53	1.99	72	97	124
4	**3** (Hf)	0, 20	–[i]	–	–	–	–	–

[a] *Polymerization conditions*. Toluene = 30 mL, M(Ti, Zr, Hf) = 20 μmol, dried MAO = 8.0 mmol, propylene = 1 atm, 30 min.
[b] Activity in kg-PP · mol-M^{-1} · h^{-1}.
[c] Determined by GPC using universal calibration.
[d] Number of polymer chains calculated from yield and M_n.
[e] Determined by ^{13}C NMR.
[f] Determined by DSC.
[g] See [14b] in detail.
[h] Not detected.
[i] Not polymerized.

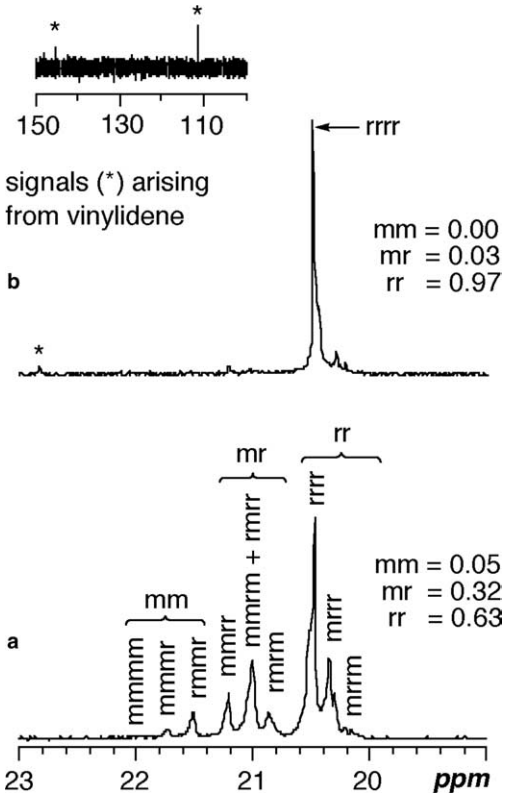

Fig. 4. 125 MHz ^{13}C NMR spectra of methyl region of polypropylenes obtained with **1** and **2**–dried MAO: (a) **1** in entry 1; (b) **2** in entry 3.

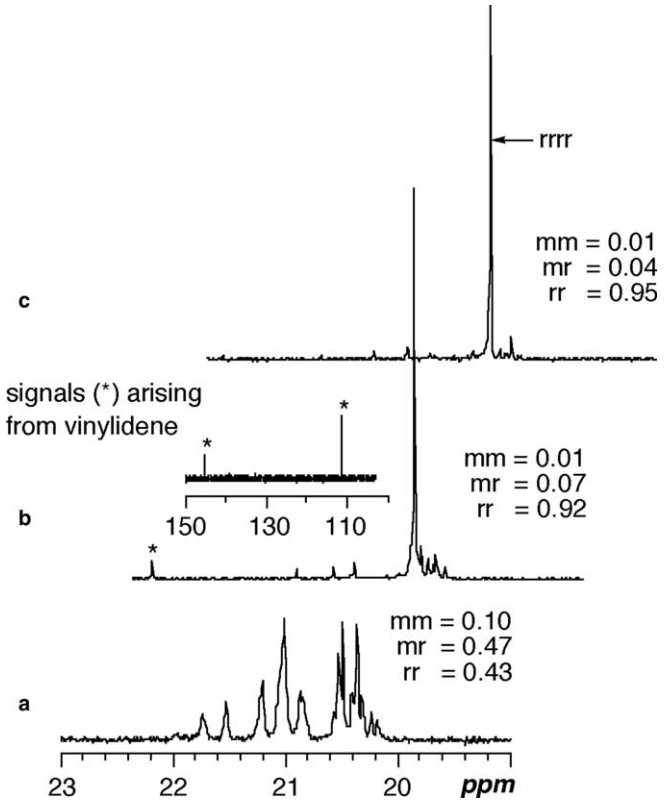

Fig. 5. 125 MHz ^{13}C NMR spectra of methyl region of polypropylenes obtained with **1**, **2** and **3**–$HNMe_2PhB(C_6F_5)_4$: (a) **1** in entry 5; (b) **2** in entry 6; (c) **3** in entry 7.

All the complexes showed activity for propylene polymerization under these conditions. **1** showed the highest activity and gave the highest M_n with the broadest M_w/M_n. On the other hand, in the case of **2** and **3**, the M_n value was lower and M_w/M_n value was narrower than that of **1**. Although the N value in entry 5 was almost the same with the number of the Ti complex employed, the consumption rate of propylene, which was measured by a mass flow meter, was stopped within 9 min. The results indicate that this catalyst system was deactivated immediately. The N value in entry 6 was 4.5 times higher than the number of the Zr complex employed, while the N value in entry 7 was about 1/10 of the number of Hf complex employed. These results indicated that chain transfer reaction occurred in the **2** system, while the initiation efficiency was very low in the **3** system.

Fig. 5 displays the ^{13}C NMR spectra of the methyl region of the PPs obtained with **1**–**3**. The **1**–$HNMe_2PhB(C_6F_5)_4$ system gave slightly syndiotactic-enriched PP (rr = 43%), while the **2** and **3**–$HNMe_2PhB(C_6F_5)_4$ systems gave highly syndiotactic PPs (rr > 94%).

The steric pentad fractions of methyl group in main chain determined by ^{13}C NMR spectroscopy. The results are summarized in Table 5.

The pentad values indicate that the stereospecificity depends on the center metal used. Fujita et al. studied propylene polymerization with the group 4

Table 4
Results of propylene polymerization with [*t*-BuNSiMe$_2$Flu]MMe$_2$–HMe$_2$NPhB(C$_6$F$_5$)$_4$ catalyst[a]

Entry	Catalyst	Time (min)	A[b]	M_n[c] ($\times 10^3$)	M_w/M_n[c]	N[d] (μmol)	rr[e] (%)	T_m[f] (°C)
5	**1** (Ti)	9	143.3	19.8	3.22	43	43	–[g]
6	**2** (Zr)	20	22.7	1.68	1.26	180	92	115
7	**3** (Hf)	30	0.56	3.06	1.48	3.7	95	129

[a] *Polymerization conditions.* Toluene = 30 mL, M(Ti, Zr, Hf) = B = 40 μmol, $^{i}Bu_3Al$ = 800 μmol, propylene = 1 atm, 20 °C.
[b] Activity in kg-PP · mol-M^{-1} · h^{-1}.
[c] Determined by GPC using universal calibration.
[d] Number of polymer chains calculated from yield M_n.
[e] Determined by ^{13}C NMR.
[f] Determined by DSC.
[g] Not detected.

Table 5
^{13}C NMR analysis of polypropylenes obtained with **1**, **2** and **3**

Pentad distributions	**1** (Ti) (entry 5)	**2** (Zr) (entry 6)	**3** (Hf) (entry 7)
mmmm	0.01	0.00	0.00
mmmr	0.04	0.00	0.00
rmmr	0.05	0.01	0.01
mmrr	0.10	0.03	0.03
mmrm + rmrr	0.26	0.04	0.01
rmrm	0.11	0.00	0.00
rrrr	0.20	0.82	0.86
mrrr	0.19	0.09	0.09
mrrm	0.04	0.01	0.00

bis[*N*-(3-*tert*-butylsalicylidene)anilinato]complexes–$Ph_3CB(C_6F_5)_4$–$^iBu_3Al$ systems [13a] and the group 4 bis[*N*-(3-*tert*-butylsalicylidene)-2,3,4,5,6-pentafluoroanilinato] complexes – MAO systems. [13b] They found that the mm triads in the former systems increased in the following order: Ti (mm = 22.9%) < Zr (mm = 45.8%) < Hf (mm = 69.0%). On the other hand, in the latter systems, the Ti complex gave a highly syndiotactic (rr = 87%) polymer, but the Zr and Hf complexes gave the non-stereoregular polymers.

The **2**–$HNMe_2PhB(C_6F_5)_4$ and **3**–$HNMe_2PhB(C_6F_5)_4$ systems gave high "rrrr" pentad values of 82% and 86%, respectively, with the stereo defects of "rmmr" arising from the miss selection of prochiral face and "rmrr" arising from the site epimerization. The "rmmr" values are similar in both systems, while the "rmrr" value in the **3**–$HNMe_2PhB(C_6F_5)_4$ system is lower than that in the **2**–$HNMe_2PhB(C_6F_5)_4$ system. These stereo defect values indicate that the higher syndiospecificity of the **3**–$HNMe_2PhB(C_6F_5)_4$ system can be ascribed to the suppression of the site epimerization.

On the other hand, the **1**–$HNMe_2PhB(C_6F_5)_4$ system gave the lowest "rrrr" value of 20%. The reason why the **1** system gave the lowest stereospecificity PP should be as follows. Chien and co-workers [30a] reported the synthesis of isotactic–atactic stereoblock PP with a stereorigid chiral *ansa*-titanocene. They proposed the mechanism where the polymer chain migrates between two different coordination sites (isospecific and non-stereospecific sites) [30]. The results suggest that the chain migration should more easily occurred in *ansa*-titanocene than in the corresponding Zr or Hf derivative. The high "rmrr" value (mrmm + rmrr = 26%) supports this assumption. The "rmmr" value in the **1** system is also higher than those of the other systems, which indicates the low enantioselectivity of **1**.

Since the bond angle of N(1)–M(1)–C(4) in **1** (Ti) is larger than those of **2** (Zr) and **3** (Hf) (cf. Section 3.1), the steric hindrance around active species is smaller in the case of **1** and hence the enantioselectivity of **1** should be lower than those of **2** and **3**.

Razavi et al. reported that the change of hapticity or the variation of bond order during polymerization should be considered in the syndiotactic specific polymerization of propylene with metallocene catalysts because the haptotropy and ring-slippage can influence the electronic and steric properties of the active site [31]. A plausible change of the coordination mode in the present complexes is shown in Fig. 6. If this isomerization occurs more frequently in **1** than in **2** or **3**, the syndiospecificity of **1** should also be decreased due to the C_1-symmetric structure of the isomers.

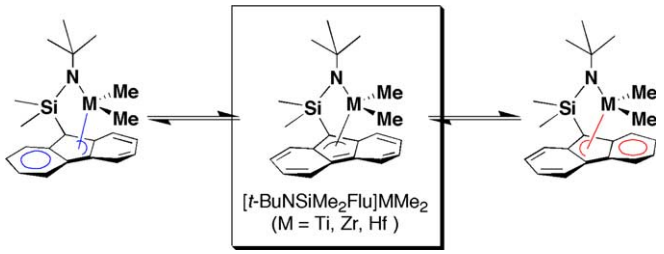

Fig. 6. A plausible scheme of ring-slippage in group 4 *ansa*-fluorenylamidodimethyl complexes.

The signals assignable to vinylidene and *n*-propyl chain end groups (Fig. 5(b)) indicate that β-H elimination also occurred by **2** activated with $HNMe_2PhB(C_6F_5)_4$. The signals arising from regioirregular units were not observed in all the polymers regardless of the complex used, even when $HNMe_2PhB(C_6F_5)_4$ was used as a cocatalyst.

4. Conclusion

A series of group 4 dimethyl complexes with a *tert*-butyl(dimethylfluorenylsilyl)amido ligand were synthesized with a facile method and the fluorenyl ligand was found to coordinate to center metal in a η^3–manner irrespective of center metal employed. The Ti complex activated with dried MAO at 0 °C gave the syndiotactic-enriched PP with narrow M_w/M_n, whereas the complex gave almost atactic PP with broad M_w/M_n when activated with $HNMe_2PhB(C_6F_5)_4$ at 20 °C. The Zr complex gave a low-molecular weight syndiotactic PP with vinylidene and *n*-propyl chain end groups irrespective of the cocatalyst employed. The Hf complex polymerized propylene only when activated by $HNMe_2PhB(C_6F_5)_4$. Although this system showed the lowest catalytic activity, the produced PP had the highest syndiotacticity. It was found that catalytic activity and the stereospecificity were strongly dependent on both the center metal of the *ansa*-fluorenylamidodimethyl complex and the cocatalyst employed.

Acknowledgements

We thank Tosoh-Finechem Co., Ltd. for donating MAOs. We thank Dr. Yuushou Nakayama and Mr. Mitsuhiro Okada for useful discussion and EI-MS study (Hiroshima University). We also acknowledge support from the New Energy and Industrial Technology Development Organization (NEDO) under the Ministry of Economy, Trade and Industry (METI), Japan, granting the project on "Nanostructured Polymeric Materials" in the "Material Nanotechnology Program" since 2001.

Appendix A. Supplementary data

Crystallogaphic data have been deposited with the Cambridge Crystallogaphic Data Centre, CCDC Nos. 274545, 274546 and 274547 for complexes **1**, **2** and **3**, respectively. Copies of data are obtained free of charge on application to CCDC, 12 Union Road, Cambridge CB2 1EZ, UK (fax: +44 01223 336033; e-mail: deposit@ccdc.cam.ac.uk). Supplementary data associated with this article can be found, in the online version, at doi:10.1016/j.jorganchem.2005.08.027.

References

[1] (a) H.-H. Brintzinger, D. Fischer, R. Mülhaupt, B. Rieger, R.M. Waymouth, Angew. Chem. Int. Ed. Engl. 34 (1995) 1143;
(b) G.J.P. Britovsek, V.C. Gibson, D.F. Wass, Angew. Chem. Int. Ed. Engl. 38 (1999) 428;
(c) V.C. Gibson, S.K. Spitzmesser, Chem. Rev. 103 (2003) 283.

[2] (a) P.J. Shapiro, E. Bunel, W.P. Schaefer, J.E. Bercaw, Organometallics 123 (1990) 1649;
(b) P.J. Shapiro, W.D. Cotter, W.P. Schaefer, J.A. Labinger, J.E. Bercaw, J. Am. Chem. Soc. 116 (1994) 4623.

[3] J. Okuda, Chem. Ber. 123 (1990) 1649.

[4] Eur. 416815 A2 (1991) and U.S. 401345 (1990), Dow Chemical Corporation, invs.: J.C. Stevens, F.J. Timmers, D.R. Wilson, G.F. Schmidt, P.N. Nickias, R.K. Rosen, G.W. Knight, S.Y. Lai, Chem. Abstr. 115 (1991) 93163m.

[5] (a) U.S. 5026798 (1991), Exxon Chemical Corporation, inv.: J.M.A. Canich, Chem. Abstr. 118 (1993) 60284k;
(b) , U.S. 5055438 (1991), Exxon Chemical Corporation, inv.:J.M.A. Canich, Chem. Abstr. 118 (1993) 60283;
(c) , WO 9319103 (1993), Exxon Chemical Corporation, inv.:H.W. Turner, G.G. Halatky, J.M.A. Canich, Chem. Abstr. 120 (1994) 271442q.

[6] For example, review articles for olefin polymerization with CpA catalysts; A.L. McKnight, R.M. Waymouth, Chem. Rev. 98 (1998) 2587, and references therein.

[7] (a) F.G. Sernetz, R. Mülhaupt, R.M. Waymouth, Macromol. Chem. Phys. 197 (1996) 1071;
(b) F.G. Sernetz, R. Mülhaupt, F. Amor, T. Eberle, J. Okuda, J. Polym. Sci., Part A: Polym. Chem. 35 (1997) 1571;
(c) F.G. Sernetz, R. Mülhaupt, J. Polym. Sci., Part A: Polym. Chem. 35 (1997) 2549;
(d) G. Xu, Macromolecules 31 (1998) 2395;
(e) G. Xu, E. Ruckenstein, Macromolecules 31 (1998) 4724;
(f) G. Xu, D. Cheng, Macromolecules 34 (2001) 2040.

[8] (a) J.M.A. Canich, U.S. 5504169, Exxon Chemical Corporation, inv. (1996);
(b) A.L. McKnight, M.A. Masood, R.M. Waymouth, D.A. Straus, Organometallics 16 (1997) 2879;
(c) L. Resconi, I. Camurati, C. Grandini, M. Rinaldi, N. Mascellani, O. Traverso, J. Organomet. Chem. 664 (2002) 5;
(d) C. De Rosa, F. Auriemma, O. Ruiz de Ballesteros, L. Resconi, A. Fait, E. Ciaccia, I. Camurati, J. Am. Chem. Soc. 125 (2003) 10913, and references therein.

[9] J. Okuda, F.J. Schattenmann, S. Wokadlo, W. Massa, Organometallics 14 (1995) 789.

[10] H. Hagihara, T. Shiono, T. Ikeda, Macromolecules 30 (1997) 4783.

[11] (a) A. Razavi, V. Bellia, Y. De Brauwer, K. Hortmann, M. Lambrecht, O. Miserque, L. Peters, S. Van Belle, in: W. Kaminsky (Ed.), Metalorganic Catalysts for Synthesis and Polymerization, Springer-Verlag, Berlin, 1999, p. 236, and references therein;
(b) A. Razavi, U. Thewalt, J. Organomet. Chem. 621 (2001) 267;
(c) V. Busico, R. Cipullo, F. Cutillo, G. Talarico, A. Razavi, Macromol. Chem. Phys. 204 (2003) 1269.

[12] T. Shiomura, T. Asanuma, N. Inoue, Macromol. Rapid Commun. 17 (1996) 9.

[13] (a) J. Saito, M. Onda, S. Matsui, M. Mitani, R. Furuyama, H. Tanaka, T. Fujita, Macromol. Rapid Commun. 23 (2002) 1118;
(b) H. Makio, Y. Tohi, J. Saito, M. Onda, T. Fujita, Macromol. Rapid Commun. 24 (2003) 894, and references therein.

[14] (a) H. Hagihara, T. Shiono, T. Ikeda, Macromolecules 31 (1998) 3184;
(b) T. Hasan, A. Ioku, K. Nishii, T. Shiono, T. Ikeda, Macromolecules 34 (2001) 3142;
(c) K. Nishii, T. Matsumae, E.O. Dare, T. Shiono, T. Ikeda, Macromol. Chem. Phys. 205 (2004) 363.

[15] (a) D. Balboni, G. Prini, M. Rinaldi, L. Resconi, Am. Chem. Soc. Polym. Prep. 41 (2000) 456;
(b) D. Balboni, I. Camurati, G. Prini, L. Resconi, S. Galli, P. Mercandelli, A. Sironi, Inorg. Chem. 40 (2001) 6588;
(c) C. Grandini, I. Camurati, S. Guidotti, N. Mascellani, L. Resconi, I.E. Nifant'ev, I.A. Kashulin, P.V. Ivchenko, P. Mercandelli, A. Sironi, Organometallics 23 (2004) 344, and references therein.

[16] D.W. Carpenetti, L. Kloopenburg, T.J. Kupec, J.L. Petersen, Organometallics 15 (1996) 1572.

[17] T. Higashi, Program for absorption correction, Rigaku Corp., Tokyo, Japan, 1995.

[18] TEXSAN; Crystal Structure Analysis Package, ver. 1. 11; Rigaku Corp., Tokyo, Japan, 2000.

[19] International Tables for X-ray Crystallography, vol. 4, Kynoch Press, Birmingham, 1975.

[20] (a) G.M. Sheldrick, SHELXS-86: Program for crystal structure determination, University of Göttingen, Göttingen, Germany, 1986;
(b) G.M. Sheldrick, SHELXL-97: Program for crystal structure refinement, University of Göttingen, Göttingen, Germany, 1997.

[21] P.T. Beurskens, G. Admiraal, G. Beurskens, W.P. Bosman, S. Garcia-Granda, R.O. Gould, J.M.M. Smits, C. Smykalla, The DIRDIF program system, Technical Report of the Crystallography Laboratory, University of Nijmegen, Nijmegen, The Netherland, 1992.

[22] G. Xu, Macromolecules 31 (1998) 2395.

[23] The crystallographic data of [^{t}BuNSiMe$_2$Cp*]TiMe$_2$ complex: $C_{17}H_{33}NSiTi$, F.W. $= 327.44$ g mol^{-1}, triclinic, space group *Pnma*, $a = 11.868(2)$, $b = 13.398(2)$, $c = 12.232(1)$ Å, $V = 1945.0(5)$ Å^3, $Z = 4$, $D_c = 1.118$ g cm^{-3}, $R = 0.0840$, $R_w = 0.211$, for 1669 independent reflections with $I > 2\sigma(I)$. Selected bond lengths are as follows: Ti(1)–C(3) = Ti(1)–C(5) = 2.350 Å; Ti(1)–C(4) = 2.283 Å; Ti(1)–C(6) = Ti(1)–C(7) = 2.463 Å.

[24] (a) E. Kirillov, L. Toupet, C.W. Lehmann, A. Razavi, S. Kahlal, J.-Y. Saillard, J.-F. Carpentier, Organometallics 22 (2003) 4038;
(b) E. Kirillov, L. Toupet, C.W. Lehmann, A. Razavi, J.-F. Carpentier, Organometallics 22 (2003) 4467, and references therein.

[25] M.H. Lee, J.-W. Hwang, Y. Kim, J. Kim, Y. Han, Y. Do, Organometallics 18 (1999) 5124.

[26] W.J. Evans, T.S. Gummersheimer, T.J. Boyle, J.W. Ziller, Organometallics 13 (1994) 1281.

[27] L.J. Irwin, S.A. Miller, J. Am. Chem. Soc. 127 (2005) 9972.

[28] H.G. Alt, K. Föttinger, W. Milius, J. Organomet. Chem. 572 (1999) 21.

[29] (a) S. Gentil, M. Dietz, N. Pirio, P. Meunier, J.C. Gallucci, F. Gallou, L.A. Paquette, Organometallics 21 (2002) 5162;
(b) S. Deisenhofer, T. Feifel, J. Kukral, M. Klinga, M. Leskelä, B. Rieger, Organometallics 22 (2003) 3495, and references therein.

[30] (a) D.T. Mallin, M.D. Rausch, Y.-G. Lin, S. Dong, J.C.W. Chien, J. Am. Chem. Soc. 112 (1990) 2030;
(b) G.W. Coates, Chem. Rev. 100 (2000) 1223, and references therein.

[31] A. Razavi, D. Baekelmans, V. Debrwer, K. Hortmann, M. Lambrecht, O. Miserque, M. Slawinski, L. Peters, S. Van Belle, in: T. Sano, T. Uozumi, H. Nakatani, M. Terano (Eds.), Progress and Development of Catalytic Olefin Polymerization, Technology and Education Publishers, Tokyo, 2000, p. 176, and references therein.